14th International Conference on Structural Safety and Reliability - ICOSSAR'25
1-6 June, 2025 - Los Angeles California, USA
R. Ghanem, E. Johnson, S. Masri and A. Olivier (Eds)

Development and Response Validation of a Bi-Directionally Tunable Rigid-Body-Swinging and Horizontal-Spring Hybrid Tuned Mass Damper in a Full-Scale Model

YUKI SHIMIZU*[1] AND MASAYUKI KOHIYAMA[2]

[1] Graduate School of Science and Technology, Keio University

[2] Department of System Design Engineering, Faculty of Science and Technology, Keio University

Key words: Tuned Mass Damper, Optimal Damping Ratio, Optimal Frequency Ratio.

1 INTRODUCTION

Tuned mass dampers (TMDs) have been widely implemented to suppress disturbances of high-rise buildings [1–3]. Notable examples include the TMD in Taipei 101 [4] and the retrofitting of a 55-story high-rise building in Tokyo, Japan [5]. As an advanced version of this, a bidirectional tuned mass damper (BTMD) has been proposed, which is capable of controlling vibration modes with different natural frequencies in the two horizontal directions. Sone et al. [6] proposed a TMD with a two-phase support mechanism to achieve a compact and low-friction design. The system effectively mitigated vibrations from earthquakes and strong winds by combining multistage rubber bearings (MRBs) and linear motion bearings (LMBs). LMBs minimize friction under small MRB deformations while providing support during large deformations, thereby preventing MRB buckling.

Previous studies [6] have introduced BTMDs capable of bidirectional tuning. However, challenges remain in developing a BTMD suitable for practical application in full-scale buildings that also enables bidirectional "re-tuning" to adapt to changes in the natural period of the building over time. This study proposes a novel rigid body swing and horizontal spring oscillation tuned mass damper (RH-TMD) designed to accommodate buildings with different natural frequencies in two horizontal directions. The RH-TMD controls vibrations through horizontal springs connected to the mass, while allowing the entire TMD to sway perpendicular to the spring's vibration direction, thereby enabling bidirectional control.

Numerical simulations of a 31-story building model [7] were conducted to examine the feasibility of the proposed RH-TMD by checking the maximum displacement of the device under assumed ground motion. In addition, experiments were also conducted using a small-scale specimen to evaluate its performance. The RH-TMD was mounted on a single-layer test building model, and its performance was evaluated through shaking-table experiments and compared with that of a pendulum-type TMD with a single-rod suspension, which is capable of tuning in only one direction.

Based on the results of the above-mentioned experiments and analyses, we demonstrate that, while conventional TMDs can be tuned in only one direction, the RH-TMD can be tuned in two directions simultaneously, thereby eliminating the need to install the equipment in both directions. This makes the system lightweight and cost-effective, and further enhances the

seismic performance of high-rise buildings, making RH-TMD a promising alternative to conventional TMD systems.

2 DESCRIPTIONS OF THE RH-TMD

The proposed RH-TMD (Figure 1) can synchronize with different natural periods in the two horizontal directions through two types of motion: the overall swaying of the TMD (Figure 2(a)) and the rolling motion caused by the horizontal spring vibrations of the mass with wheels (Figure 2(b)). To reduce the TMD height, the strong axis direction (x-direction), corresponding to the shorter natural period of the target building, is controlled by the swaying motion, while the weak-axis direction (y-direction) is controlled by the rolling motion. The damping mechanism of the RH-TMD utilizes a rotary damper.

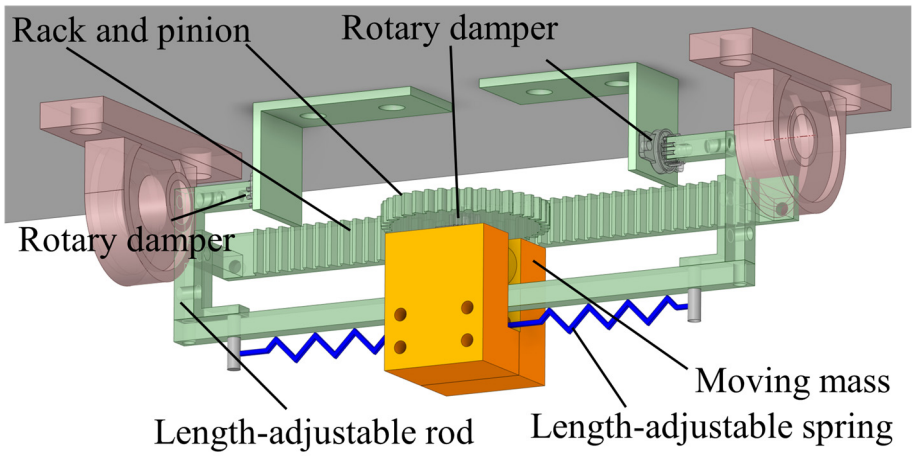

Figure 1: Overview of the RH-TMD

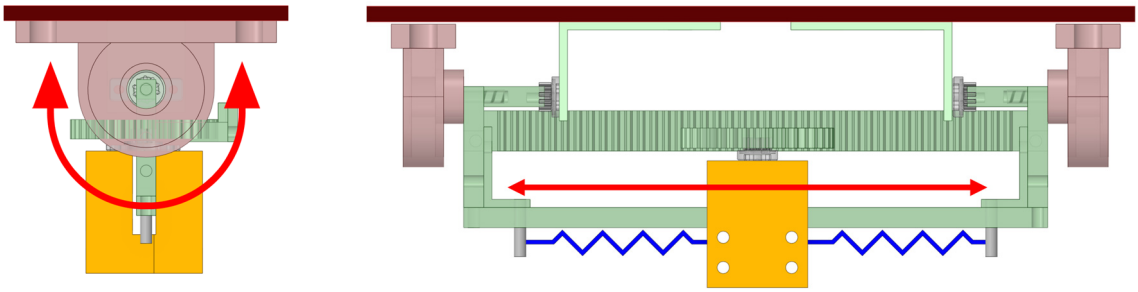

(a) Swing mechanism (b) Rolling mechanism

Figure 2: Schematic view of the RH-TMD

3 NUMERICAL ANALYSIS OF A 31-STORY MODEL WITH RH-TMD

3.1 Fifty-story building model

To examine the response reduction performance of the proposed RH-TMD, we conducted a numerical analysis using a mass–spring–damper model of a 31-story building from Yaguchi and Kurino [7] with plan dimensions of 40 m × 40 m, a total height of 31 stories, and a story height of 4 m. An RH-TMD was installed on the top floor of the model.

In this study, the model was designed such that every 10 stories shared the same mass. The mass of each floor and the stiffness of each story is listed in Table 1. As indicated in the table, the different stiffnesses were considered in the *x*- and *y*-directions. The design of the TMD was based on the approach proposed by Warburton [8], which minimizes the RMS of the displacement response of a building under white-noise acceleration ground motion. The vibration characteristics of the building are listed in Table 2, and the mode shapes are shown in Figure 3.

Table 1: Mass and stiffness of the 31-story building model

Block	Mass [×10^5 kg]	Stiffness [×10^9 N/m]	
		x-direction	*y*-direction
1st–6th stories	8.710	1.757	0.988
7th–12th stories	8.710	1.581	0.890
13th–18th stories	8.710	1.405	0.791
19th–24th stories	8.710	1.230	0.692
25th–31st stories	8.710	1.054	0.593

Table 2: Vibration characteristics of the 31-story building model

	Modal Mass [×10^7 kg]	Modal stiffness [×10^8 N/m]	Natural Frequency [Hz]	
			x-direction	*y*-direction
1st	1.239	0.54	0.333	0.250
2nd	1.176	4.11	0.941	0.706
3rd	1.216	11.63	1.557	1.168

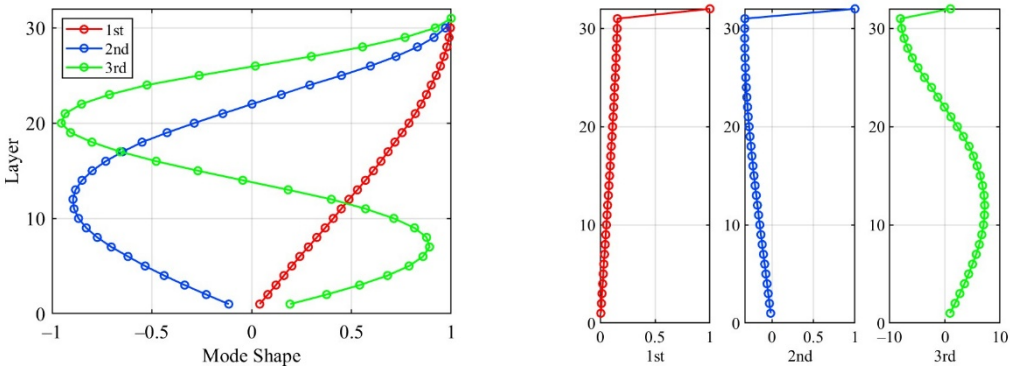

(a) Building (b) Building and BTMD

Figure 3: Mode shapes of the 31-story model

3.2 Input ground motions

The input ground motions used in the analysis were three design ground motions of a rare seismic event (approximate return period of 500 years) stipulated in Item (4) of Notification No. 1461 issued by the Minister of Construction of Japan in 2000 (hereafter, notification wave) with phase characteristics of JMA Kobe wave, Hachinohe wave, and random number. Figures 4 and 5 show the acceleration time-history waves and acceleration response spectra of the input ground motions. The ground motions were input at 45° relative to the *x*-axis.

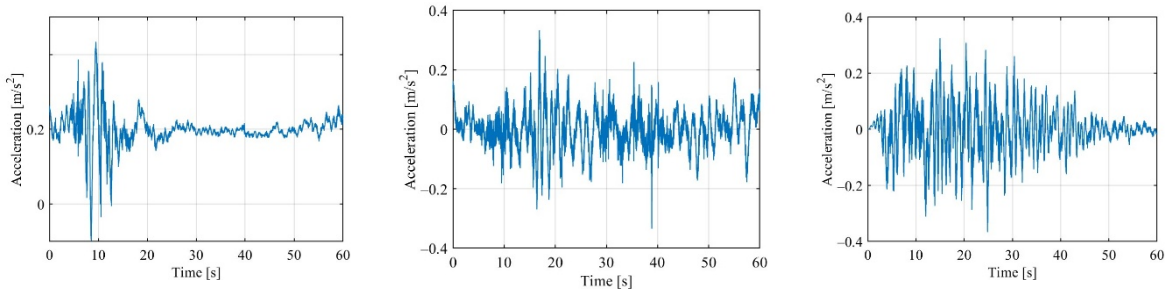

(a) Kobe wave phase (b) Hachinohe wave phase (c) Random phase

Figure 4: Time-history waveforms of input design seismic motions

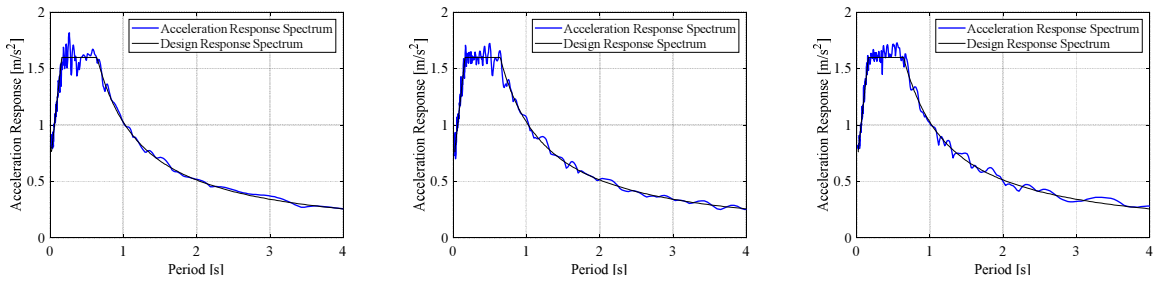

(a) Kobe wave phase (b) Hachinohe wave phase (c) Random phase

Figure 5: Acceleration response spectra of input design seismic motions (damping ratio: 5%)

3.3 Analysis results

Using the building model and input ground motions mentioned in the previous sections, time-history response analysis was conducted with the assumption of linear elastic response. A fourth-order Runge–Kutta method was employed for time integration. Figures 6–8 show the peak and RMS responses of each story in the *x* and *y*-directions. The RH-TMD exhibits better reduction performance than the simple TMD. The peak displacement of the TMD mass relative to the top floor is 0.56 m in the *x*-direction and 0.80 m in the *y*-direction, confirming that it is within a scalable range for application in full-scale buildings.

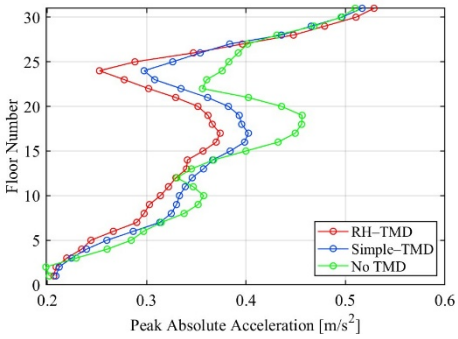

(a) Peak absolute acceleration (*x*-direction)

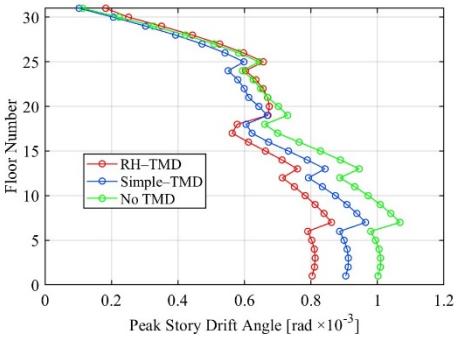

(b) Peak story drift angle (*x*-direction)

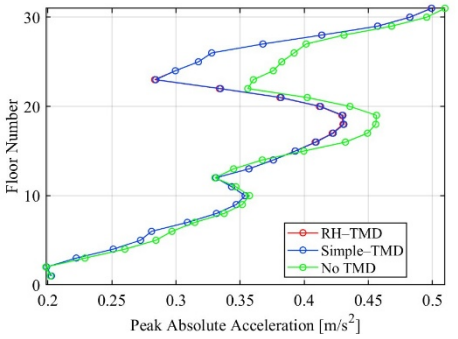

(c) Peak absolute acceleration (*y*-direction)

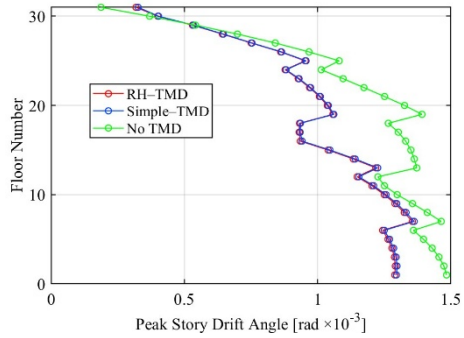

(d) Peak story drift angle (*y*-direction)

Figure 6: Responses under the notification wave with the Kobe wave phase characteristics

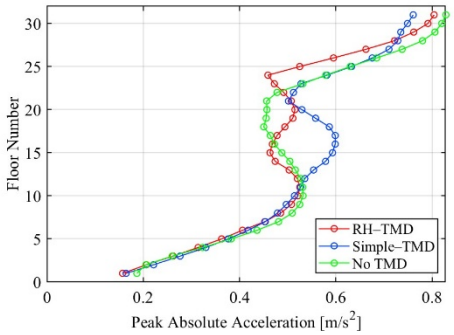

(a) Peak absolute acceleration (*x*-direction)

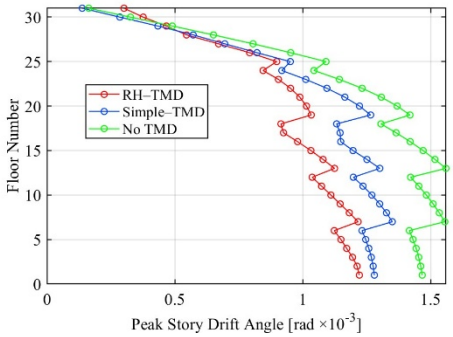

(b) Peak story drift angle (*x*-direction)

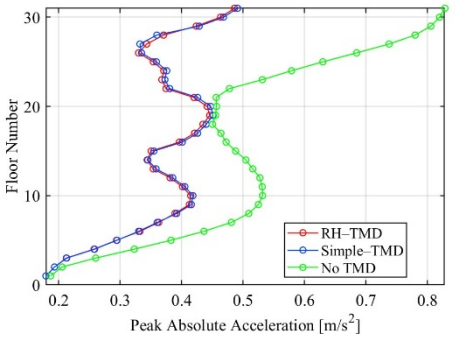

(c) Peak absolute acceleration (*y*-direction)

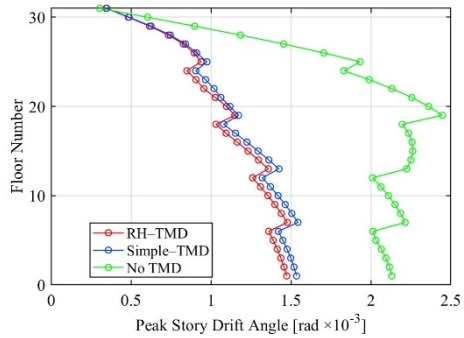

(d) Peak story drift angle (*y*-direction)

Figure 7: Responses under the notification wave with the Hachinohe wave phase characteristics

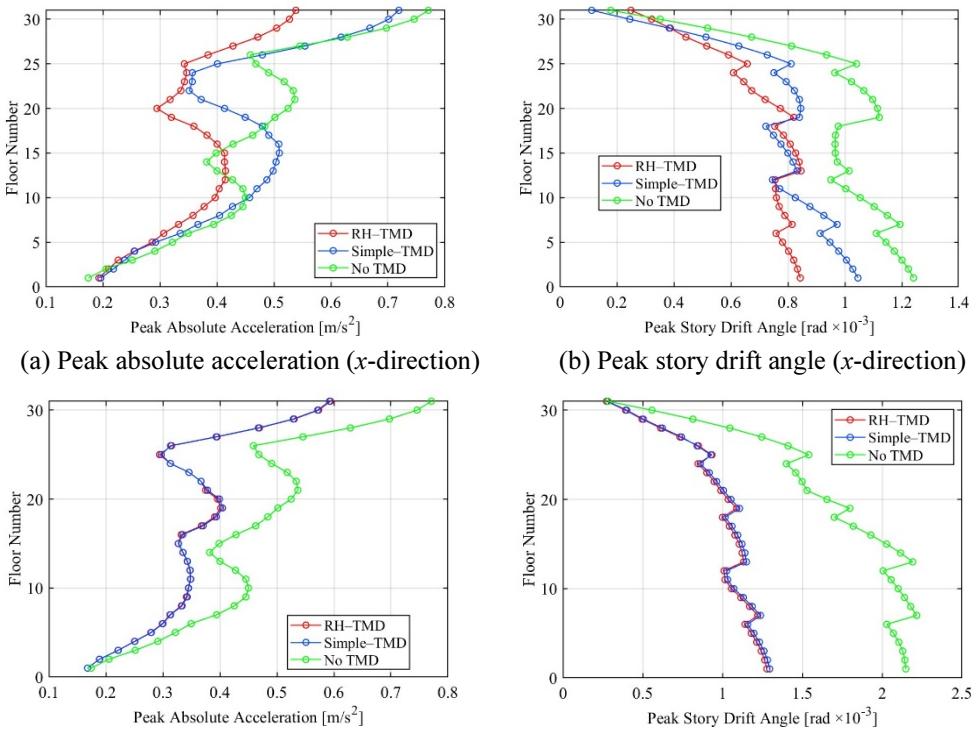

(a) Peak absolute acceleration (*x*-direction) (b) Peak story drift angle (*x*-direction)

(c) Peak absolute acceleration (*y*-direction) (d) Peak story drift angle (*y*-direction)

Figure 8: Responses under the notification wave with random phase characteristics.

4 SHAKING TABLE TEST OF A SINGLE-LAYER SPECIMEN WITH RH-TMD

4.1 TMD parameters

To minimize building response, we adopted the optimization method proposed by Warburton [8], which minimizes the root mean square (RMS) of the displacement response of the building to the ground motion of white noise acceleration. The influence of building damping is reported to be small [7]; hence, the optimal frequency ratio Ω_{opt} and damping ratio $\zeta_{\mathrm{t,opt}}$ were determined without considering the effects of building damping. The optimal parameters were derived using the mass ratio μ between the building and the TMD, as follows:

$$\mu = \frac{m_{\mathrm{t}}}{m_{\mathrm{s}}} \tag{1}$$

$$\Omega_{\mathrm{opt}} = \frac{\omega_{\mathrm{t,opt}}}{\omega_{\mathrm{s}}} = \sqrt{1-\mu/2}\,/(1+\mu) \tag{2}$$

$$\zeta_{\mathrm{t,opt}} = \sqrt{\frac{\mu(1-\mu/4)}{4(1+\mu)(1-\mu/2)}}, \tag{3}$$

where $\omega_{\mathrm{s}} = \sqrt{m_{\mathrm{s}}/k_{\mathrm{s}}}$; $\zeta_{\mathrm{t}} = c_{\mathrm{t}}/(2\sqrt{m_{\mathrm{t}}k_{\mathrm{t}}})$; m_{s} and k_{s} are the mass and stiffness of the specimen, respectively; and m_{t}, k_{t}, and c_{t} are the mass, stiffness, and damping coefficient of the TMD, respectively. In contrast to the RH-TMD, a simple TMD can only tune its frequency and damping coefficient in one direction, either *x* or *y*. In this experiment, the cable length l was

adjusted to tune the TMD in the weak-axis direction (*y*-direction), where the displacement response is larger.

4.2 Target building and similarity ratios for the specimen

We selected the 31-story building introduced in Section 3.1 as the target structure. Table 3 shows the similarity ratios between the full-scale target building and the reduced-scale single-layer building specimen based on previous studies [9] with respect to natural periods and frequencies of the target building and specimen.

Table 3: Similarity ratios of natural periods and frequencies

		Target building	Specimen	Similarity ratio (target building/specimen)
Slab dimensions		40 m × 40 m	0.4 m × 0.4 m	$\lambda = 100$
Natural period	**Strong axis**	3 s	0.319 s	$\lambda^{\frac{1}{2}} = \sqrt{100}$
	Weak axis	4 s	0.491 s	$\lambda^{\frac{1}{2}} = \sqrt{100}$
Natural frequency	**Strong axis**	0.333 Hz	3.13 Hz	$\lambda^{-\frac{1}{2}} = 1/\sqrt{100}$
	Weak axis	0.25 Hz	2.03 Hz	$\lambda^{-\frac{1}{2}} = 1/\sqrt{100}$

The acceleration ratio was set to 1. When a specimen is fabricated with a similarity ratio of 100:1, the similarity ratio of the natural periods becomes $\sqrt{100}:1$.

4.3 Fabrication of the specimen

(1) Single-layer building specimen

A single-layer building specimen with different natural frequencies in the *x*- and *y*-directions was designed and fabricated to investigate the vibration control performance of the RH-TMD tuned to a target building with different natural frequencies in the two horizontal directions. The specimens comprised columns made of extra-strong duralumin YH75; the other components were made of aluminum alloy A5052. All components were connected using bolts and nuts. For a simple TMD, copper plates for the eddy current damper were positioned beneath the slab of the building specimen and supported by a post. Figures 9 present an overview of the single-layer building specimen.

Figure 9: Overview of the single-layer building specimen

Free vibration experiments were conducted in both *x*- and *y*-directions to determine the vibration characteristics of the fabricated single-layer building specimens. Table 4 presents the identified vibration characteristics of the building specimen.

Table 4: Vibration characteristics of the building specimen

Direction	Sample size	Period [s]		Frequency [Hz]	Damping ratio [%]	
		Mean	Standard deviation	Mean	Mean	Standard deviation
x	3	0.319	0.0006	2.28	1.06	0.108
y	3	0.491	0.0004	1.50	1.65	0.021

(2) RH-TMD and Simple TMD

The mass component in the RH-TMD was fabricated using stainless steel SUS303, and its external dimensions were 25 mm × 30 mm × 31 mm. Its weight could be adjusted by attaching metal plates. It has two wheels inside; four miniature ball bearings with an outer diameter of 10 mm and inner diameter of 5 mm are inserted to minimize friction during wheel rotation. The axles inserted into the ball bearings had a diameter of 5 mm, whereas the contact surface of the wheel with the rail had a diameter of 12 mm. The wheels were designed to have a larger diameter to maximize the distance traveled per rotation, thereby reducing friction. A rotary damper rotating horizontally and a large gear meshed with a rack were mounted on top of the mass component. The spring for controlling the rolling direction of the mass component was designed to have the shortest possible natural length for maintaining a compact TMD. It was connected to the mass component via a screw running through the rail. The dimensions of the rail were 5 mm × 5 mm × 140 mm. The rigid bar suspending the rail was equipped with a rack and a rotary damper, which were used to generate damping in the *y*-direction by meshing with the gear. A rigid bar was mounted on the bearing units to minimize friction in the swaying direction. This configuration reduced the frictional resistance of the swaying mechanism.

The mass of the building specimen, including the joint parts at the bottom of the columns, was 9176 g. The effective mass of the TMD differed in the *x*- and *y*-directions when the weight of the gear, angle, and rail were considered. Additionally, as the natural period of the mass–spring system in the *y*-direction was adjusted by changing the mass, the optimal parameters varied based on the number of attached metal plates. The optimal parameters were determined using Equations (1)–(3). This established the target tuning period and damping ratio. To determine the natural periods and damping ratios of the RH-TMD in the *x*- and *y*-directions, free vibration experiments were conducted. Two triaxial accelerometers were mounted to avoid offsetting the center of gravity. Free-vibration experiments were subsequently conducted. The two accelerometers weighed 20 g, and the experiment was designed such that the mass section including the accelerometers accounted for 5% of the total mass of the building specimen. The RH-TMD used three weights with a total mass of 196 g and a pendulum length of 31 mm.

The external dimensions of the mass component cube of the simple TMD were 31 mm × 31 mm × 28 mm. A hook screw was inserted into the top surface of the cube to connect it to a suspension rod, and a ⌀22 mm permanent magnet, which composed an eddy current damper, was fixed to the bottom surface with countersunk screws. The material of the mass component was stainless steel SUS303, which was chosen because of its high density and low magnetic susceptibility. The hook screw was used for suspending the mass. The mass of the rod, including

the simple TMD and accelerometers, was 197 g. The optimal parameters were determined by using Equations (1)–(3) and setting the target tuning period and damping ratio. The pendulum length was 46 mm, and the gap was 1 mm.

The natural frequencies and damping ratios obtained by free-vibration experiments are summarized in Table 5.

Table 5: Natural frequencies and damping ratios of the RH-TMD and simple TMD

TMD	Direction	Frequency [Hz]	Damping ratios [%]
RH-TMD	*x*	3.05	5.09
	y	2.00	11.4
Simple TMD	*x* and *y*	1.99	7.40

4.4 Experiment results

Acceleration sensors were attached to the single-layer building specimen to measure the acceleration response in three cases: with no TMD, with the simple TMD, and with the RH-TMD. The measured acceleration data were processed using a bandpass filter with sixth-order Butterworth characteristics and a passband frequency of 0.8–50 Hz. The resulting acceleration and displacement waveforms for the three cases were compared. The acceleration was measured for approximately 80 s. The response reduction performance was evaluated by comparing the peak and RMS responses calculated from the acceleration time history. The RMS response was calculated as the RMS of the data from 5 s to 80 s. The displacement waveform was obtained by simulating the response of a seismometer with a natural period of 10 s and damping ratio of $1/\sqrt{2}$. For the shaking table experiments, a San-Esu permanent magnet biaxial shaking table (SPT2D-10K-85L-10T) was used, and the notification wave (Figure 10) was input to the building specimen.

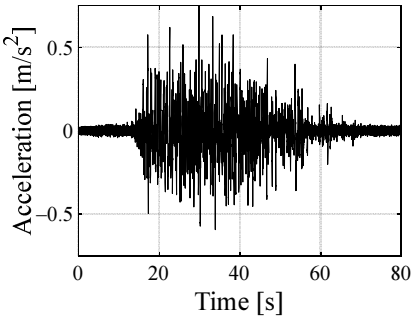

Figure 10: Input motion used in the shaking table experiments

The response-time histories are shown in Figure 11. The response reduction performance improves in the following order: no TMD, simple TMD, and RH-TMD for the response convergence rate, peak response, and RMS response. In the *y*-direction, both the RH-TMD and simple TMD were tuned to this direction; therefore, they show equivalent response reduction performance.

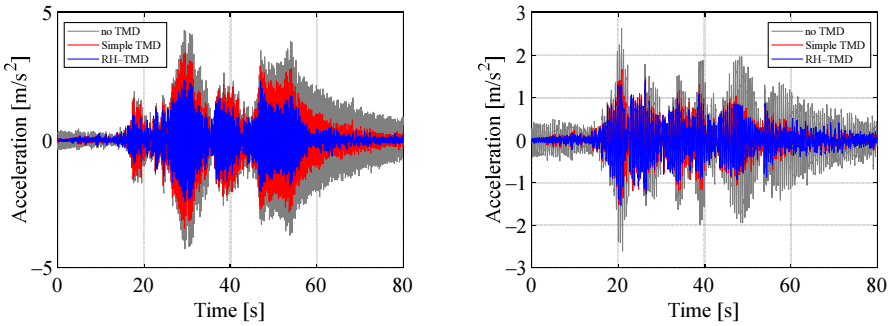

(a) *x*-direction (b) *y*-direction

Figure 11: Acceleration response time-history under the notification wave

A performance comparison was conducted using the seismic motion simulated in the *x*- and *y*-directions. The input seismic motion was the notification wave, compressed by a factor of $1/\sqrt{100}$ in time according to the similarity rule explained in Section 4.2. Figure 12 presents the comparison of the responses. In the *x*-axis direction, the RH-TMD exhibited the best performance in terms of absolute acceleration response convergence rate, peak response, and RMS response. In the *y*-axis direction, it was confirmed under the notification wave that the performance of the simple TMD and the RH-TMD was approximately the same.

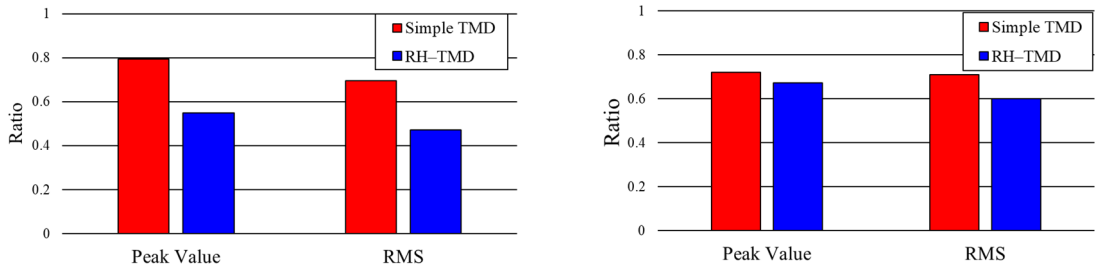

(a) *x*-direction (b) *y*-direction

Figure 12: Comparison of responses

6 CONCLUSIONS

A novel TMD, the RH-TMD, was proposed for vibration control of buildings with different stiffnesses in the two horizontal directions, utilizing horizontal spring oscillations and rigid body swaying. To predict the responses of the building and the TMD, numerical analysis assuming moderate seismic ground motion was conducted using a 31-story model, and experimental analysis was performed using a scaled model representing an actual building. The response reduction performance was compared with that of a conventional simple TMD, which can be tuned in only one direction. In both analyses, in the *x*-direction, where the simple TMD was not tuned, the RH-TMD exhibited significantly better response reduction performance in terms of peak and RMS displacement. In the *y*-direction, both dampers demonstrated effective response reduction performance. Under simultaneous excitation in both directions, the RH-TMD consistently outperformed the simple TMD.

The challenges associated with such analyses include ensuring adaptability to the cases of strong ground motion where structural members cause plastic deformation, inducing changes in vibration characteristics, and securing sufficient stroke of the TMD mass. In addition, the design of members for full-scale applications of the proposed approach has not been extensively examined in this study; this will be addressed in future research. Although these challenges remain, the proposed BTMD can be a promising alternative to conventional TMDs because it is a cost-effective and lightweight system that can the seismic resilience of high-rise buildings at different natural frequencies in two horizontal directions.

REFERENCES

[1] Brock, J.E. A note on the damped vibration absorber. *J. Appl. Mech.* (1946) **13**(4):A284.
[2] Den Hartog, J.P. *Mechanical Vibrations*, 4th ed. McGraw-Hill, New York, (1956).
[3] Rana, R. and Soong, T.T. Parametric study and simplified design of tuned mass dampers. *Eng. Struct.* (1998) **20**(3):193–204.
[4] Gutierrez Soto, M. and Adeli, H. Tuned mass dampers. *Arch. Comput. Methods Eng.* (2013) **20**(4):419–431.
[5] Nakai, T., Kurino, H., Yaguchi, T., and Kano, N. Control effect of large tuned mass damper used for seismic retrofitting of existing high-rise building. *Jpn. Archit. Rev.* (2019) **2**(3):269–286.
[6] Sone, T., Ogino, K., Kamoshita, N., Muto, K., Ide, Y., Murata, K., Hamaguchi, H., and Yamamoto, M. Experimental verification of a tuned mass damper system with two-phase support mechanism. *Jpn. Archit. Rev.* (2019) **2**(3):250–258.
[7] Yaguchi, T. and Kurino, H. Study on stroke control strategy of seismic control structure utilizing large-weight sub-system as dynamic mass damper. *J. Struct. Constr. Eng.* (2017) **82**(738):1201–1211. (in Japanese)
[8] Warburton, G.B. Optimum absorber parameters for various combinations of response and excitation parameters. *Earthq. Eng. Struct. Dyn.* (1982) **10**(3):381–401.
[9] Tabatabaiefar, H.R. and Mansoury, B. Detail design, building and commissioning of tall building structural models for experimental shaking table tests. *Struct. Des. Tall Spec. Build.* (2016) **25**(8):357–374.